

Generation and performance of special quasirandom structures for studying the elastic properties of random alloys: Application to Al-Ti

Johann von Pezold,^{*} Alexey Dick, Martin Friák, and Jörg Neugebauer
Max-Planck-Institut für Eisenforschung GmbH, D-40237 Düsseldorf, Germany

(Received 20 November 2009; published 17 March 2010)

The performance of special-quasirandom structures (SQSs) for the description of elastic properties of random alloys was evaluated. A set of system-independent 32-atom-fcc SQS spanning the entire concentration range was generated and used to determine C_{11} , C_{12} , and C_{44} of binary random substitutional AlTi alloys. The elastic properties of these alloys could be described using the set of SQS with an accuracy comparable to the accuracy achievable by statistical sampling of the configurational space of $3 \times 3 \times 3$ (108 atom, C_{44}) and $4 \times 4 \times 4$ (256 atom, C_{11} and C_{12}) fcc supercells, irrespective of the impurity concentration. The smaller system size makes the proposed SQS ideal candidates for the *ab initio* determination of the elastic constants of random substitutional alloys. The set of optimized SQS is provided.

DOI: [10.1103/PhysRevB.81.094203](https://doi.org/10.1103/PhysRevB.81.094203)

PACS number(s): 62.20.de, 61.43.Bn

I. INTRODUCTION

Hardness and ductility are two of the key parameters for the design and characterization of novel materials. These quantities largely depend on the elastic properties of the material, as described by the elastic stiffness tensor. Efficient and reliable methods are therefore required for the prediction of these quantities. The elastic constants of pure phases can nowadays be routinely calculated (at least at 0 K) using electronic structure methods, while the prediction of the elastic properties of low-symmetry systems, such as random alloys, is less straight forward. In particular, the faithful reproduction of randomness in these structures poses a significant challenge. A naive atomistic description of random alloys based on a randomly generated impurity distribution requires a considerable configurational space and can hence only be achieved using large supercells, which render standard electronic structure methods unfeasible. Instead three alternative approximations are generally employed: the coherent potential approximation (CPA), the cluster expansion (CE) method and special-quasirandom structures (SQSs). In the CPA the random distribution of impurity atoms is described in the framework of the mean-field approximation—a concentration-dependent effective potential is found by averaging the scattering properties of the alloy constituents, which reproduces the electronic properties of the actual alloy when placed on every matrix site.^{1,2} The CPA works well for the description of coherent alloys consisting of chemical species of similar size, which induce only small lattice relaxations, but it is not well suited for alloys of sizable lattice mismatch, in which relaxation effects may be significant. The CE method allows to take lattice relaxations into account, and is based on the assumption that the energy (or any other scalar property) of a system can be expanded in terms of a set of well-chosen structural motives (figures). The expansion parameters are typically obtained by fitting the CE Hamiltonian to *ab initio* electronic structure calculations.³ Using this parametrization the system sizes required for a faithful representation of the random distribution of impurities within the alloy matrix can be readily accessed.⁴ In SQS randomness is introduced by mimicking as closely as pos-

sible the correlation functions of an infinite random alloy within a finite supercell.⁶ Total energies^{7,8} and thermodynamic properties^{7,9} have been found to be similarly well described by the different methods, while for the determination of elastic properties the CPA has been the method of choice so far, despite the recent extension of the CE method to the description of tensorial properties.^{5,10} The performance of SQS to describe elastic properties has not been systematically evaluated hitherto.

We have therefore determined the elastic constants of random substitutional binary alloys over the entire concentration range using a set of system-independent 32-atom-fcc SQS. As model system we use AlTi alloys, which are also of considerable technological interest for high temperature applications in the automotive and aerospace industries.¹¹ In order to assess the accuracy of the obtained results, the elastic constants have also been calculated by statistical sampling of an ensemble of local structures, as represented by a set of supercells. To ensure convergence large supercells containing up to 4000 atoms had to be employed. The description of a large number of such extended systems by standard electronic structure methods is impractical at present. A semi-empirical EAM-type potential was therefore adopted for the simulations throughout this study. Based on the elastic constants determined using this potential we (i) evaluate the suitability and performance of SQS to obtain accurate elastic constants at minimum system sizes, (ii) estimate the residual error bars due to this approximation and (iii) provide an explicit set of SQS structures over the entire concentration range.

II. METHODS

A. SQS generation

The generation of SQS for a given alloy should ideally be based on knowledge of the physical interactions in that particular system, since these interactions define the choice of the proper structural motives (figures) in the SQS scheme. While the CE methodology does allow to choose such motives using, e.g., genetic algorithms,¹² such a search requires

a significant number of supporting DFT calculations to parametrize the CE Hamiltonian. The SQS identified using this approach are system-dependent and a complete reparametrization of the CE Hamiltonian is therefore required for every new system. Instead of considering such system-optimized SQS we propose in this paper a set of generic, system-independent SQS, which should perform well for all systems in which long-range interactions of both chemical and elastic nature are not significant.

Binary SQS have been generated over the entire concentration range for cubic fcc cells containing 32 atoms, employing the ATAT package.¹³ This choice of cell shape allows us to describe the elastic constants C_{11} , C_{12} , and C_{44} , employing only a single supercell, as described in the next section. To estimate the quality of a particular arrangement of species σ , we have adapted the ATAT package to include a new definition of the error function. Our new error function quantifies the deviation of the averaged correlation function of a particular structure from the corresponding correlation function of a truly infinite random alloy of the same composition,

$$\epsilon(\sigma) = \sum_f \frac{D_f}{(k\bar{d}_f)^n} \left| \overline{\prod_f(\sigma)} - \langle \overline{\prod_f} \rangle_R \right|. \quad (1)$$

Equation (1) is based on the formalism in Ref. 6, according to which the atomic lattice is discretized into its component figures $f=(k,m)$, where k is the number of vertices in the figure, and m is the maximum distance spanned by the figure edge in units of nearest-neighbor shells; D_f is the symmetry defined multiplicity of a figure, and $\overline{\prod_f(\sigma)}$ is the lattice average of the products of the spin variables, which take values of $+1$ or -1 depending on which chemical element occupies a given lattice site, and $\bar{d}_f = \frac{1}{N} \sum_{i,j} d_{ij}$ is the mean distance between vertices i,j in a figure. The corresponding lattice averaged correlation function of an ideal, infinite random alloy is known analytically and given by $\langle \overline{\prod_f} \rangle_R = (2x-1)^k$ for many-body ($k>0$) figures, where x is the impurity concentration.⁶ We note that in contrast to previously proposed schemes for the SQS error function,^{14,15} the definition given by Eq. (1) accounts for the span of figures f in Cartesian coordinates (by introducing \bar{d}_f) instead of relying on the atomic shell number which gives only implicit information on the real-space distance between vertices. Our ansatz assumes that the correlation-errors stemming from figures with a large number of vertices and/or with large interaction distances are less critical than those with small k and \bar{d}_f , which makes the generated SQS particularly suited for systems without pronounced long-range effects. Parameter n in Eq. (1) defines the magnitude of the damping for different figures. We have found that for $1 < n < 5$ the SQS search results in identical arrangements σ_{SQS} , and have therefore chosen $n=2$.

For a binary system consisting of n_A and n_B atoms in the supercell and neglecting possible degeneracy due to symmetry the number of possible arrangements scales according to $N_{\text{conf}} = (n_A + n_B)! / n_A! n_B!$. For large systems ($n_A + n_B \geq 32$) and $n_A/n_B \sim 1$ this quickly results in a configurational space

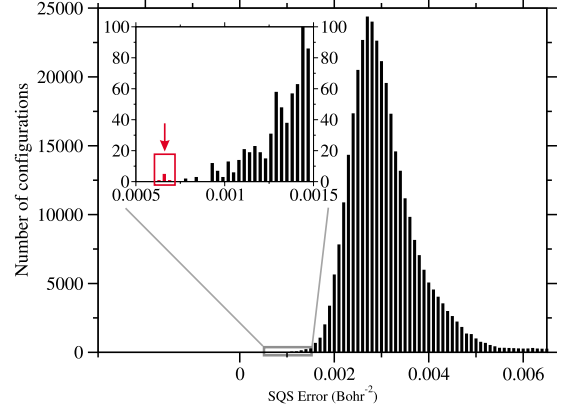


FIG. 1. (Color online) Generation of the SQS for the $\text{Al}_{50}\text{Ti}_{50}$ random alloy. The configurational space is sampled by more than 3×10^5 randomly chosen configurations, which ensures that the quality of the five most favorable SQS candidates (indicated by the red arrow) as measured by Eq. (1) does not vary by more than 5%. The complete configurational space for a given alloy composition spans more than 6×10^8 structures.

spanning 10^9 and more configurations, which renders the problem computationally unfeasible. Therefore, only for systems of small configurational space (low concentration) each distinct configuration has been considered explicitly. For systems with large configurational space we have performed a Monte Carlo search for the optimal SQS by randomly sampling the configurational space of 3×10^5 configurations until the quality of the five most favorable SQS candidates as measured by Eq. (1) did not vary by more than 5%, as shown in Fig. 1. We note, that such an approach allows for natural parallelization of the search process since the choice of each test structure is completely independent of the previous steps.

Employing the ansatz described above we have generated SQS using the following set of figures f : all two-body figures spanning distances up to the ninth atomic shell, all three-body figures spanning up to the maximum intervertex distance of five shells, and all four- and five-body figures spanning up to fourth and second-atomic shells, respectively $\{f\} = \{(k=2, m \leq 9), (k=3, m \leq 5), (k=4, m \leq 4), (k=5, m \leq 2)\}$. These settings result in 66 symmetry nonequivalent figures f that represent the interatomic interactions on the fcc lattice. The optimum configurations derived using this approach are summarized in the Appendix and are available for download from our website.¹⁶

B. Standard supercell approach

In order to estimate the error bars in the elastic constants determined using the SQS, the corresponding elastic properties were also calculated using the standard supercell approach involving a *randomly generated* impurity distribution within the alloy matrix. The accuracy of this approach depends on the configurational space within the supercell and can hence be improved by increasing the supercell size. In this study the size of the supercells was systematically in-

creased from $2 \times 2 \times 2$ (32 atom) up to $10 \times 10 \times 10$ (4000 atom) fcc supercells, in order to determine a converged set of elastic constants to compare the SQS results to. Moreover, to account for statistical fluctuations of the calculated data arising from the random nature of the impurity distribution scheme, we considered ten independent impurity distributions for every impurity concentration within the different supercells.

C. Determination of elastic constants

Elastic constants were determined from the second derivative of the internal energy with respect to the strain tensor (ϵ). Due to the low symmetry of random alloys all 21 independent elastic constants have to be determined in order to fully describe the elastic properties of these systems. However, for the sake of simplicity we focused on the three principle elastic constants of cubic systems (C_{11} , C_{12} , and C_{44}), which can be determined from the energetic response of the system to monoclinic and orthorhombic distortions, given by

$$\epsilon_{mono} = \begin{pmatrix} 0 & \delta/2 & 0 \\ \delta/2 & 0 & 0 \\ 0 & 0 & \delta^2/(4 - \delta^2) \end{pmatrix} \quad (2)$$

and

$$\epsilon_{ortho} = \begin{pmatrix} \delta & 0 & 0 \\ 0 & -\delta & 0 \\ 0 & 0 & \delta^2/(1 - \delta^2) \end{pmatrix}, \quad (3)$$

respectively, where δ corresponds to the magnitude of the strain. In this study δ was varied from -0.01 to $+0.01$ in steps of 0.002 . The energy change corresponding to these distortions is given by

$$E_{mono}(\delta) = VC_{44}\delta^2 + O[\delta^4] \quad (4)$$

and

$$E_{ortho}(\delta) = V(C_{11} - C_{12})\delta^2 + O[\delta^4], \quad (5)$$

respectively. By fitting the calculated energy-strain relationship by a third-order polynomial and taking the second derivative, C_{44} could be directly determined from Eq. (4). C_{11} and C_{12} were determined by combining the coefficient obtained for the $(C_{11} - C_{12})$ term in Eq. (5) with the expression relating these elastic constants to the bulk modulus (B), given by

$$B = (C_{11} + 2C_{12})/3. \quad (6)$$

The bulk modulus, in turn, was obtained by calculating the energy-volume dependence of the system and fitting it to the Murnaghan equation of state.¹⁷ Due to the lack of symmetry of the structures considered here, the three possible (orthogonal) monoclinic/orthorhombic distortions are inequivalent.

This was accounted for by defining mean elastic constants, $\overline{C_{ij}}$, which were determined by averaging over the three individual elastic constants, obtained from the inequivalent distortions along the three orthogonal directions.

D. Computational details

The elastic constants of the AlTi system were calculated at the equilibrium, relaxed volume, using the ITAP Molecular Dynamics (IMD)¹⁸ program. Ionic degrees of freedom were allowed to relax throughout. The interatomic interactions were described by a well-established EAM potential for the AlTi system by Zope *et al.*,¹⁹ who fitted the potential functions to a database of experimental properties and *ab initio* energies of bulk Al and Ti, as well as of γ -TiAl. The predicted structural, energetic and elastic properties of these phases are generally in good agreement with available experimental²⁰/*ab initio* data. Moreover, the properties of the $D0_{19}$ -Ti₃Al phase are again rather well reproduced,¹⁹ even though the Ti₃Al phase was not part of the fitting target, suggesting that the potential is reasonably transferable. It is therefore anticipated that the elastic constants determined for the random solid solutions considered in this study should also be reasonably described. Moreover, absolute accuracy is only of secondary importance for the purpose of this study, as we are not primarily aiming to describe the AlTi system as such, but rather strive to evaluate the applicability of SQS for the description of elastic constants of random alloys in general. Since any shortcoming of the potential will equally affect the elastic constants determined using the SQS and those obtained for the randomly generated impurity distributions, our conclusions should not be majorly affected by the limited accuracy of the interaction parameters. However, it is noted that the truncation of the interaction radius of the EAM potential at a cutoff radius of 5.77 \AA will obscure any long-ranged, chemical interactions. Our results are therefore expected to hold for systems in which such interactions are small.

III. RESULTS

The results for the $\overline{C_{11}}$, $\overline{C_{12}}$, and $\overline{C_{44}}$ elastic constants are summarized in Fig. 2. All three elastic constants exhibit a strongly nonlinear dependence on the impurity concentration with a global maximum for a Ti concentration of 0.5 . This maximum stiffness of $\text{Al}_{0.5}\text{Ti}_{0.5}$ solid solutions is attributed to the strength of the Al-Ti bond, which is also reflected in the stability of the γ -(L1₀) TiAl intermetallic phase. For $\overline{C_{11}}$ a shallow local minimum is found at a Ti concentration of 0.9 .

The description of the elastic constants by the standard supercell approach improves significantly as the dimensions of the system are increased. Hence, irrespective of the nature of the elastic constant, the $2 \times 2 \times 2$ supercells exhibit consistently the largest scatter, while hardly any scattering is observed in the elastic constants determined using the $10 \times 10 \times 10$ supercells. In fact only a minor reduction in the scatter of $\overline{C_{ij}}$ is observed as the cubic cell dimensions are increased beyond six, suggesting that the configurational

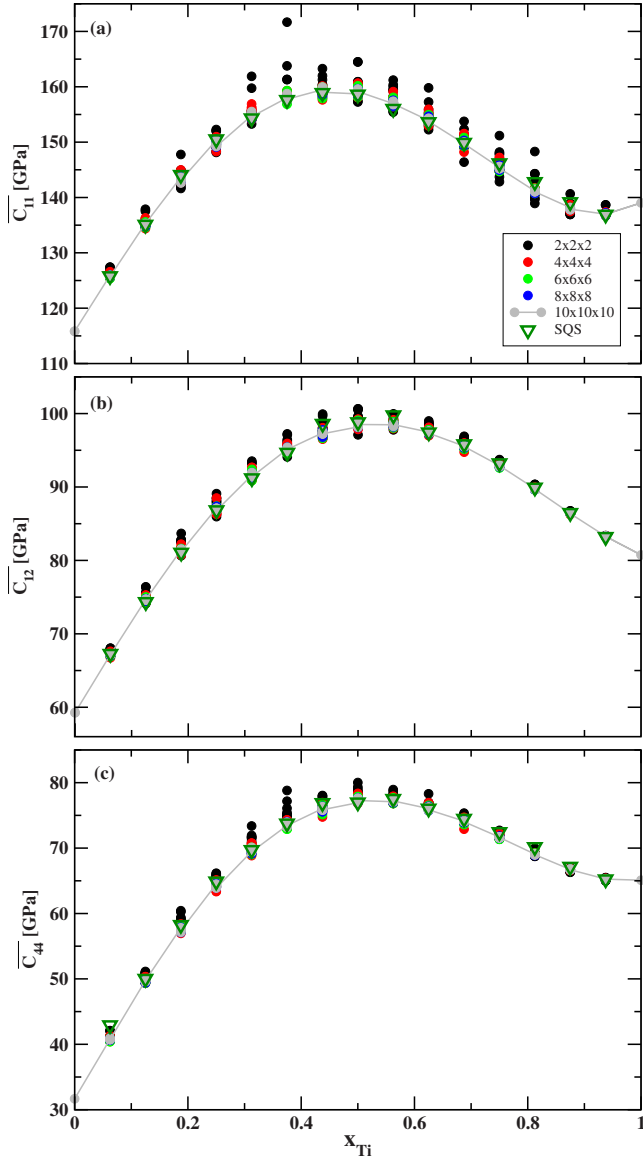


FIG. 2. (Color online) (a) $\overline{C_{11}}$, (b) $\overline{C_{12}}$, and (c) $\overline{C_{44}}$ as a function of the Ti fraction within the AlTi solid solution and the dimensions of the supercells used to determine the elastic constants within the standard supercell approach. The corresponding elastic constants determined using the SQS are indicated by triangles. The continuous gray line serves as guide to the eyes only.

space within conventional $6 \times 6 \times 6$ supercells is in principle sufficiently large to allow for a converged description of random alloys by randomly generated impurity distributions.

However, an average of the results obtained for the ten independent impurity distributions within the $10 \times 10 \times 10$ supercells ($\overline{C_{ij}}$) was considered as the gold standard for all three elastic constants investigated over the entire concentration range and used as a reference in the subsequent analysis. The largest deviations from $\overline{C_{ij}}$ were found for Ti concentrations ranging between 0.2 and 0.8, which is attributed to the increased configurational space as the impurity concentration approaches 0.5, for which the configurational space reaches a maximum.

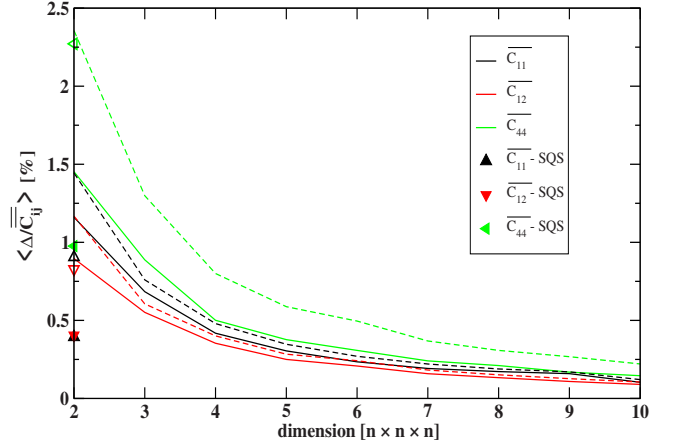


FIG. 3. (Color online) Average absolute deviation, Δ , of the calculated elastic constants with respect to $\overline{C_{ij}}$, determined using the standard supercell approach (lines) and the SQS (triangles). Continuous lines (filled triangles) correspond to the absolute deviation of the averaged elastic constants ($\overline{C_{ij}}$), while dashed lines (open triangles) depict the absolute deviation of the individual elastic constants (C_{ij}).

In contrast, the deviation of the SQS-based elastic constants from $\overline{C_{ij}}$ is essentially concentration independent for all three elastic constants investigated, which suggests that the increased randomness of solid solutions in the concentration range around 0.5 is well reproduced by these structures. Moreover, the SQS-based elastic constants deviate significantly less from $\overline{C_{ij}}$ than the corresponding elastic constants obtained using randomly generated impurity distributions within $2 \times 2 \times 2$ supercells—in fact the SQS-based elastic constants fall within the scatter of the $10 \times 10 \times 10$ supercells in most cases.

For a more quantitative assessment of the accuracy of the elastic constants obtained using the SQS and the standard supercell approach, the average absolute deviation, Δ , with respect to $\overline{C_{ij}}$ was determined, as shown in Fig. 3. The $\overline{C_{11}}$ and $\overline{C_{12}}$ calculated using the SQS reproduce the corresponding $\overline{C_{ij}}$ to within 0.5% over the entire concentration range, while $\overline{C_{44}}$ is reproduced to within 1% by the SQS. This level of accuracy is comparable to the accuracy achievable using $4 \times 4 \times 4$ ($\overline{C_{11}}$ and $\overline{C_{12}}$) and $3 \times 3 \times 3$ ($\overline{C_{44}}$) supercells in the standard supercell approach. Assuming $O(N^2)$ scaling for electronic structure methods and accounting for the need of a statistical average over ten independent impurity distributions in the standard supercell approach, the increased accuracy of the SQS-based elastic constants at a decreased system size can be correlated with a reduction in CPU time of two ($\overline{C_{44}}$) to three ($\overline{C_{11}}$ and $\overline{C_{12}}$) orders of magnitude. Moreover, the sampling error of less than 1% achievable using the SQS is below the typical error in density functional theory (DFT) calculations. This suggests that the proposed set of SQS will allow for the determination of elastic properties of random alloys to within the accuracy of the exchange-correlation functional used, provided long-range interactions are negligible.

Figure 3 also suggests that the three orthogonal, symmetry-inequivalent monoclinic/orthorhombic distortions

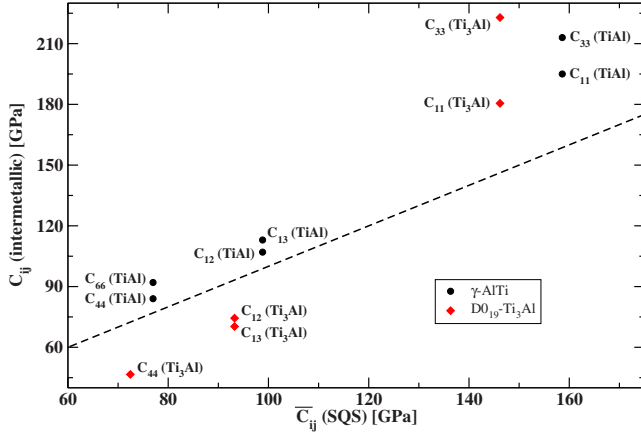


FIG. 4. (Color online) Effect of randomness on the elastic constants of the AlTi system. The matching of the previously determined elastic constants (Ref. 19) of the intermetallic γ -TiAl and the $D0_{19}$ -Ti₃Al phases to the \overline{C}_{ij} of the SQS proposed in this study, is described in the text. The dashed line indicates equality between the SQS-derived and intermetallic elastic constants.

have to be taken into account explicitly when determining elastic constants of random alloys: averaging over the elastic constants obtained from the three symmetry-inequivalent monoclinic/orthorhombic distortions reduces the average absolute deviation in the obtained results by up to 60% (SQS, C_{44}). The gain in accuracy is most pronounced for the $2 \times 2 \times 2$ supercells. This is attributed to the significant elastic anisotropy in these supercells, resulting from the small configurational space within these systems.

Finally, it is interesting to consider the effect of randomness on the elastic properties of the AlTi system. To this end we compare the elastic constants of two intermetallic phases ($L1_0$ (γ)-TiAl and $D0_{19}$ -Ti₃Al) of the AlTi system that have been previously determined using the same interaction potential¹⁹ to the SQS-based elastic constants determined in this study for the corresponding Ti concentrations (0.5 and 0.75). Due to the noncubic symmetry of the intermetallic phases, more than three symmetry-inequivalent elastic constants exist: For γ -TiAl six symmetry-inequivalent elastic constants (C_{11} , C_{12} , C_{13} , C_{33} , C_{44} , and C_{66}) have been reported, while for the Ti₃Al phase the elasticity tensor reduces to five independent elastic constants (C_{11} , C_{12} , C_{13} , C_{33} , and C_{44}). Assuming cubic symmetry for the SQS, the averaged principle elastic constants derived in this study (\overline{C}_{11} , \overline{C}_{12} , \overline{C}_{44}) could be related to the elastic constants of the intermetallic phases, as follows: $\overline{C}_{11} \rightarrow C_{11}, C_{33}$, $\overline{C}_{12} \rightarrow C_{12}, C_{13}$, and $\overline{C}_{44} \rightarrow C_{44}, C_{66}$. The corresponding elastic constants are plotted in Fig. 4.

It is noted that the elastic constants of the ordered phases deviate by as much as 50% from the corresponding SQS-based elastic constants, highlighting the need to properly account for the randomness in solid solution systems. Moreover, the deviations do not follow any obvious trend: While all the elastic constants of γ -TiAl are stiffened with respect to the \overline{C}_{ij} of the SQS, both stiffened and softened elastic constants are found in the case of the $D0_{19}$ -Ti₃Al phase. It is therefore concluded that the effect of ordering on the elastic properties of a materials system cannot be generically pre-

dicted, but depends on the exact symmetry of the ordered phase. While this conclusion is in line with physical intuition, it is noted that these results are significantly less reliable than our results pertaining to the evaluation of SQS-based elastic constants, as structures of different phases are compared, which precludes an efficient error cancellation. A study addressing this issue using a more accurate method (e.g., *ab initio* electronic structure calculations) would therefore be of interest.

IV. CONCLUSION

Using a Monte-Carlo-based search scheme we have constructed a set of system-independent 32-atom-fcc SQS covering the entire concentration range (see Appendix). This set of structures was used to evaluate the performance of SQS for the description of elastic properties. The three principle elastic constants of the fcc-based AlTi random alloys (C_{11} , C_{12} , and C_{44}) were reproduced (using a single SQS structure for every concentration) with an average deviation of less than 1% of the fully converged results obtained from randomly generated Ti distributions within a $10 \times 10 \times 10$ (4000 atoms) Al supercell. This sampling error in the SQS-based elastic constants is comparable to the average sampling error expected for randomly generated impurity distributions within $3 \times 3 \times 3$ (C_{44}) and $4 \times 4 \times 4$ (C_{11} and C_{12}) fcc supercells. The relatively small size of the proposed SQS makes them ideal candidates for the description of the elastic properties of random alloys by *ab initio* methods. The approach described here can be easily extended to construct similar sets of SQS for bcc- and hcp-based random alloys.

ACKNOWLEDGMENTS

We would like to thank David Holec from the Department of Physical Metallurgy and Materials Testing, Montanuniversität Leoben, Austria, for many fruitful discussions. J.v.P. and M.F. acknowledge funding by the Interdisciplinary Centre for Materials Simulation (ICAMS), which is supported by ThyssenKrupp AG, Bayer MaterialScience AG, Salzgitter Mannesmann Forschung GmbH, Robert Bosch GmbH, Benteler Stahl/Rohr GmbH, Bayer Technology Services GmbH and the state of North-Rhine Westphalia as well as the European Commission in the framework of the European Regional Development Fund (ERDF). Financial support of the collaborative research center SFB 761 “Stahl—*ab initio*” of the Deutsche Forschungsgemeinschaft is gratefully acknowledged by A.D.

APPENDIX

The SQS structures used in this study are given in Table I and on our website.¹⁶

TABLE I. Generic SQS for the study of elastic properties of fcc-based random alloys. A and B correspond to the two constituents of the binary alloy. Atomic positions are given as fractional coordinates within a $2 \times 2 \times 2$ (32 atom) fcc supercell. Note that SQS for concentrations greater than 0.5 can be generated by interchanging the nature of constituents A and B.

Coordinates	Concentration							
	$\frac{1}{16}$	$\frac{1}{8}$	$\frac{3}{16}$	$\frac{1}{4}$	$\frac{5}{16}$	$\frac{3}{8}$	$\frac{7}{16}$	$\frac{1}{2}$
$\frac{1}{4} \frac{1}{2} \frac{1}{4}$	B	B	B	B	B	B	A	B
$\frac{1}{4} 0 \frac{1}{4}$	B	B	B	A	B	B	B	B
$\frac{1}{2} \frac{1}{4} \frac{1}{4}$	B	B	B	B	B	B	B	B
$\frac{1}{2} \frac{3}{4} \frac{1}{4}$	B	A	A	B	A	B	A	A
$\frac{3}{4} \frac{1}{2} \frac{1}{4}$	B	B	A	B	B	B	B	A
$\frac{3}{4} 0 \frac{1}{4}$	A	A	B	B	B	B	A	A
$0 \frac{1}{4} \frac{1}{4}$	B	B	B	B	B	B	B	B
$0 \frac{3}{4} \frac{1}{4}$	B	B	B	B	A	A	B	A
$\frac{1}{4} \frac{1}{4} \frac{1}{2}$	B	B	B	B	B	B	A	B
$\frac{1}{4} \frac{3}{4} \frac{1}{2}$	B	B	B	B	B	B	A	A
$\frac{1}{2} \frac{1}{2} \frac{1}{2}$	B	B	B	B	A	B	B	A
$\frac{1}{2} 0 \frac{1}{2}$	B	B	B	B	B	A	A	A
$\frac{3}{4} \frac{1}{4} \frac{1}{2}$	B	B	B	A	B	B	B	B
$\frac{3}{4} \frac{3}{4} \frac{1}{2}$	B	B	A	B	B	B	A	A
$0 \frac{1}{2} \frac{1}{2}$	B	B	B	B	B	B	B	B
$0 0 \frac{1}{2}$	A	B	A	B	B	A	B	B
$\frac{1}{4} \frac{1}{2} \frac{3}{4}$	B	B	B	B	A	A	B	A
$\frac{1}{4} 0 \frac{3}{4}$	B	B	B	A	B	A	A	B
$\frac{1}{2} \frac{1}{4} \frac{3}{4}$	B	B	B	A	B	B	B	A
$\frac{1}{2} \frac{3}{4} \frac{3}{4}$	B	B	B	B	B	A	B	A
$\frac{3}{4} \frac{1}{2} \frac{3}{4}$	B	B	B	B	B	B	B	A
$\frac{3}{4} 0 \frac{3}{4}$	B	A	B	A	A	A	A	B
$0 \frac{1}{4} \frac{3}{4}$	B	B	B	A	B	A	A	B
$0 \frac{3}{4} \frac{3}{4}$	B	B	B	B	A	B	B	B
$\frac{1}{4} \frac{1}{4} 0$	B	B	B	B	B	A	B	A
$\frac{1}{4} \frac{3}{4} 0$	B	B	B	B	A	A	B	A
$\frac{1}{2} \frac{1}{2} 0$	B	B	B	A	B	B	A	B
$\frac{1}{2} 0 0$	B	B	B	B	B	A	A	A
$\frac{3}{4} \frac{1}{4} 0$	B	A	A	B	A	A	A	B
$\frac{3}{4} \frac{3}{4} 0$	B	B	A	B	A	B	B	B
$0 \frac{1}{2} 0$	B	B	B	B	A	B	B	B
$0 0 0$	B	B	B	A	B	B	A	A

*j.pezold@mpie.de

- ¹P. Soven, Phys. Rev. **156**, 809 (1967).
- ²B. L. Gyorffy, Phys. Rev. B **5**, 2382 (1972).
- ³J. M. Sanchez, F. Ducastelle, and D. Gratias, Physica A **128**, 334 (1984).
- ⁴D. B. Laks, L. G. Ferreira, S. Froyen, and A. Zunger, Phys. Rev. B **46**, 12587 (1992).
- ⁵J. Z. Liu, A. van de Walle, G. Ghosh, and M. Asta, Phys. Rev. B **72**, 144109 (2005).
- ⁶A. Zunger, S.-H. Wei, L. G. Ferreira, and J. E. Bernard, Phys. Rev. Lett. **65**, 353 (1990).
- ⁷D. D. Johnson and M. Afsar, Comput. Mater. Sci. **8**, 54 (1997).
- ⁸I. A. Abrikosov, A. V. Ruban, B. Johansson, and H. L. Skriver, Comput. Mater. Sci. **10**, 302 (1998).
- ⁹G. Ghosh, A. van de Walle, and M. Asta, Acta Mater. **56**, 3202 (2008).
- ¹⁰A. van de Walle, Nature Mater. **7**, 455 (2008).
- ¹¹M. Yamaguchi, H. Inui, and K. Ito, Acta Mater. **48**, 307 (2000).
- ¹²D. Lerch, O. Wieckhorst, G. L. W. Hart, R. W. Forcade, and S. Müller, Modell. Simul. Mater. Sci. Eng. **17**, 055003 (2009).
- ¹³A. van de Walle and G. Ceder, J. Phase Equilib. **23**, 348 (2002).
- ¹⁴K. A. Mäder and A. Zunger, Phys. Rev. B **51**, 10462 (1995).
- ¹⁵Y. Kong and B. Liu, J. Phys. Soc. Jpn. **76**, 024605 (2007).
- ¹⁶Electronic versions of the SQS can be downloaded from <http://www.mpie.de/?id=sqs>
- ¹⁷F. D. Murnaghan, Proc. Natl. Acad. Sci. U.S.A. **30**, 244 (1944).
- ¹⁸J. Stadler, R. Mikulla, and H.-R. Trebin, Int. J. Mod. Phys. C **8**, 1131 (1997).
- ¹⁹R. R. Zope and Y. Mishin, Phys. Rev. B **68**, 024102 (2003).
- ²⁰I. Ohnuma, Y. Fujita, H. Mitsui, K. Ishikawa, R. Kainuma, and K. Ishida, Acta Mater. **48**, 3113 (2000).